



Published in final edited form as:

*Neuron*. 2015 March 18; 85(6): 1332–1343. doi:10.1016/j.neuron.2015.02.019.

## Gamma rhythms link prefrontal interneuron dysfunction with cognitive inflexibility in *Dlx5/6*<sup>+/-</sup> mice

Kathleen K.A. Cho<sup>1,2,3</sup>, Renee Hoch<sup>1</sup>, Anthony T. Lee<sup>1,2,3</sup>, Tosha Patel<sup>1,2,3</sup>, John L.R. Rubenstein<sup>1</sup>, and Vikaas S. Sohal<sup>\*,1,2,3</sup>

<sup>1</sup>Department of Psychiatry, University of California, San Francisco, San Francisco, CA

<sup>2</sup>Center for Integrative Neuroscience, University of California, San Francisco, San Francisco, CA

<sup>3</sup>Sloan-Swartz Center for Theoretical Neurobiology, University of California, San Francisco, San Francisco, CA

### SUMMARY

Abnormalities in GABAergic interneurons, particularly fast-spiking interneurons (FSINs) that generate gamma ( $\gamma$ ; ~30-120 Hz) oscillations, are hypothesized to disrupt prefrontal cortex (PFC)-dependent cognition in schizophrenia. Although  $\gamma$  rhythms are abnormal in schizophrenia, it remains unclear whether they directly influence cognition. Mechanisms underlying schizophrenia's typical post-adolescent onset also remain elusive. We addressed these issues using mice heterozygous for *Dlx5/6*, which regulate GABAergic interneuron development. In *Dlx5/6*<sup>+/-</sup> mice, FSINs become abnormal following adolescence, coinciding with the onset of cognitive inflexibility and deficient task-evoked  $\gamma$  oscillations. Inhibiting PFC interneurons in control mice reproduced these deficits, whereas stimulating them at  $\gamma$ -frequencies restored cognitive flexibility in adult *Dlx5/6*<sup>+/-</sup> mice. These pro-cognitive effects were frequency-specific and persistent. These findings elucidate a mechanism whereby abnormal FSIN development may contribute to the post-adolescent onset of schizophrenia endophenotypes. Furthermore, they demonstrate a causal, potentially therapeutic, role for PFC interneuron-driven gamma oscillations in cognitive domains at the core of schizophrenia.

### INTRODUCTION

In the prefrontal cortex (PFC), rhythmic neural activity in the gamma-frequency band ( $\gamma$ ; ~30-120 Hz) is believed to play a key role in many cognitive functions (Uhlhaas and Singer, 2010).  $\gamma$  oscillations in the cortex and hippocampus are controlled by a specific class of inhibitory interneurons that can be identified based on either their fast-spiking electrophysiological properties or their expression of calcium-binding protein parvalbumin (PV) (Cauli et al., 1997; Kawaguchi and Kubota, 1993). Fast-spiking PV interneurons (FSINs) fire rhythmically at  $\gamma$  frequencies *in vivo* (Penttonen et al., 1998), and selectively

\*Correspondence to: vikaas.sohal@ucsf.edu.

#### AUTHOR CONTRIBUTIONS

KKAC, JLRR, and VSS designed experiments and wrote the manuscript. KKAC performed all of the experiments, except rule shifting in CD1 mice, which was done by TP. The generation of the *Dlx5* conditional mutants was done in part by RH. ATL generated AAV5-DlxI12b-ChR2-eYFP. KKAC and VSS analyzed the data.

activating PV interneurons at 40 Hz *in vivo* leads to a specific increase in the power of  $\gamma$  oscillations not seen with stimulation of other cell types (Cardin et al., 2009). Conversely, inhibiting PV interneurons suppresses the power of evoked  $\gamma$  oscillations *in vivo* (Sohal et al., 2009), demonstrating that PV cells play major roles in  $\gamma$  oscillations.

Altered  $\gamma$  oscillations in the PFC and other brain regions may be associated with neuropsychiatric disorders such as schizophrenia. Schizophrenia comprises positive symptoms such as hallucinations and delusions, as well as deficits in PFC-dependent cognitive domains such as attention, cognitive flexibility, working memory, and social cognition (Green, 2006). Cognitive deficits seem to represent the core of the disorder, because whereas other symptoms may enter periods of remission, cognitive symptoms persist throughout the duration of illness, correlate best with long-term functional outcome, and often precede the onset of frank psychosis (Green, 2006; Minzenberg and Carter, 2012). Unfortunately, current antipsychotic treatments are only minimally effective for cognitive symptoms (Minzenberg and Carter, 2012).

EEG recordings over human frontal cortex reveal increases in  $\gamma$  oscillations specifically during PFC-dependent tasks that require cognitive flexibility (Cho et al., 2006; Minzenberg et al., 2010). In contrast, during the same tasks, patients with schizophrenia show decreases or no change in  $\gamma$  oscillations, along with impaired performance. Studies of post-mortem brain tissue from subjects with schizophrenia have also consistently found abnormalities in cortical GABAergic interneurons derived from the medial ganglionic eminence (MGE) (Volk and Lewis, 2013), a process directed by several transcription factors including *Dlx1*, *Dlx2*, *Lhx6*, *Dlx5* and *Dlx6*. In particular, in schizophrenia, levels of GAD67 and PV are lower for PV interneurons within the PFC, and markers for GABA transporters, post-synaptic GABA receptors, and ion channels associated with PV interneurons are abnormal as well (Lewis et al., 2005; Volk and Lewis, 2013). This has led to the hypothesis that in schizophrenia, dysfunction of MGE-derived interneurons, particularly PV interneurons, results in deficient task-evoked  $\gamma$  oscillations that contribute to cognitive dysfunction and other symptoms of the disease (Lewis et al., 2005; Uhlhaas and Singer, 2010). However, it is not clear whether the alterations in interneurons observed in schizophrenia cause abnormal  $\gamma$  oscillations and thereby contribute to cognitive deficits, or whether alterations in PV interneurons and  $\gamma$  oscillations represent incidental or compensatory changes. While many studies have found important schizophrenia-related abnormalities in mutant mice with disruptions in cortical GABAergic interneurons (Belforte et al., 2010; Bissonette et al., 2014), including specific disruptions of FSINs (Carlen et al., 2012; Del Pino et al., 2013; Korotkova et al., 2010), none have reported the deficits in task-evoked  $\gamma$  oscillations that are hypothesized to mediate cognitive deficits (it is unclear whether they explicitly looked for and did not find deficient task-evoked  $\gamma$  oscillations). By contrast, NMDAR antagonists can both increase baseline  $\gamma$  oscillations and decrease sensory stimulus-evoked  $\gamma$  power (Saunders et al., 2012). Furthermore, specific aspects of GABAergic interneuron development that may contribute to the post-adolescent onset of schizophrenia remain largely unknown. Most critically, it has not yet been possible to demonstrate any causal role for interneuron-driven  $\gamma$  oscillations in cognition. Thus, the hypothesized links between

interneuron dysfunction, deficient task-evoked  $\gamma$  oscillations, and deficits in PFC-dependent cognition remain tentative at best.

Here we set out to (1) test whether the deficiency of factors which guide the development of MGE-derived interneurons can elicit key pathophysiological findings (prominent deficits in FSINs) and endophenotypes (decreased task-evoked  $\gamma$  oscillations and impaired PFC-dependent cognition) linked to schizophrenia; (2) identify developmental processes that could contribute to the post-adolescent onset of schizophrenia; and (3) directly implicate  $\gamma$ -frequency activity of PFC interneurons in cognitive domains linked to schizophrenia. To address these issues, we analyzed *Dlx5/6*<sup>+/-</sup> mutant mice. Although *Dlx5* and *Dlx6* are not known to be abnormal in schizophrenia, these homeobox transcription factors play critical roles in the development of MGE-derived cortical GABAergic interneurons. Knocking out *Dlx5/6* reduces numbers of PV interneurons without affecting numbers of interneurons belonging to other classes (Wang et al., 2010), suggesting that *Dlx5/6* are particularly important for FSIN development. While overall numbers of FS / PV interneurons are normal in both *Dlx5/6*<sup>+/-</sup> mice and schizophrenia, we hypothesized that they may exhibit functional abnormalities in *Dlx5/6*<sup>+/-</sup> mice that parallel their histochemical alterations in schizophrenia.

## RESULTS

Many factors can modulate the consequences of reductions in gene dosage in ways that depend on background strain. Therefore, although we carried out the bulk of our studies in *Dlx5/6*<sup>+/-</sup> mice on a mixed (CD1 and C57Bl/6) background, as described below, we also confirmed that major behavioral and physiological phenotypes of *Dlx5/6*<sup>+/-</sup> mice were also present in two additional lines of mice with disruptions in *Dlx5/6*: (1) *Dlx5/6*<sup>+/-</sup> mice that had been backcrossed to CD1 for at least 6 generations; (2) mice that combined heterozygosity for *Dlx6* with a forebrain GABAergic neuron-specific knockout of *Dlx5* (*Dlx112b::Cre* × *Dlx5*<sup>fl/-</sup>*Dlx6*<sup>+/-</sup>; Figure S1) and were on a different background than our *Dlx5/6*<sup>+/-</sup> mice.

### FSINs exhibit abnormal post-adolescent development in *Dlx5/6*<sup>+/-</sup> mice

To assess FSIN function in *Dlx5/6*<sup>+/-</sup> mice, we made whole-cell patch-clamp recordings from FSINs in layer 5 of medial prefrontal cortex (mPFC) in adult (P63-82) mutant mice and wild-type (WT) littermates. We visually identified interneurons for electrophysiological analyses using AAV and the *Dlx112b* enhancer to express mCherry (Lee et al. 2014). Based on electrophysiological criteria, we selected FSINs for further study (Supplemental Experimental Procedures). The well-established correspondence between PV expression and FS electrophysiological properties was maintained in *Dlx5/6*<sup>+/-</sup> and WT mice, as there were no significant differences in intrinsic properties between immunohistochemically-identified PV cells (n = 5 for each genotype) and electrophysiologically-identified FSINs (n = 16-23 for each genotype).

Based on their responses to a series of current injections, FSIN excitability was abnormal in *Dlx5/6*<sup>+/-</sup> mice (Figures 1B and 1C). Specifically, *Dlx5/6*<sup>+/-</sup> FSINs had wider spikes, higher input resistances, slower membrane time constants, and markedly elevated action

potential thresholds (WT, n = 23; *Dlx5/6*<sup>+/-</sup>, n = 16). While more subtle changes may be present in other cell types, examination of the same properties in pyramidal neurons and non-FS interneurons did not reveal any changes of comparable magnitude (Figures S2C and S2D). We also confirmed that similar differences in the intrinsic properties of adult FSINs were present in *Dlx5/6*<sup>+/-</sup> mice backcrossed to CD1 for at least 6 generations, and in *Dlx112b::Cre* × *Dlx5*<sup>fl/-</sup>*Dlx6*<sup>+/-</sup> conditional knockout mice (Figures S2E and S2F). Again, comparable deficits were not seen in pyramidal neurons or non-FS interneurons (Figures S2E and S2F).

Next, we examined whether these abnormalities in FSIN properties were age-dependent. FSIN intrinsic properties mature over several weeks (Okaty et al., 2009), and based on recordings at P16-20, P45-49, and P63-82, we observed a progressive maturation of FSIN properties – specifically, decreases in spike half-width and membrane time constant (Goldberg et al., 2011) (Figures S2A and S2B). Remarkably, FSIN intrinsic properties in *Dlx5/6*<sup>+/-</sup> mice were normal at the first two timepoints (P16-20: n = 8 mice per genotype, p = 0.5-0.9; P45-49: n = 9 WT and n = 5 *Dlx5/6*<sup>+/-</sup> mice, p = 0.4-0.9; Figure 1C). Thus, the abnormal FSIN properties we found in *Dlx5/6*<sup>+/-</sup> mice only appear during the post-adolescent period, when the normal maturation of FSIN intrinsic properties is largely complete.

We also assayed whether intrinsic FSIN deficits occur within a broader context of deficient inhibitory output by comparing evoked inhibitory currents in pyramidal neurons within the mPFC of adult *Dlx5/6*<sup>+/-</sup> and WT mice. We expressed ChR2-eYFP in interneurons using the same *Dlx112b* enhancer previously used to fluorescently label interneurons for patching. We recorded from P63-88 layer 5 pyramidal neurons while delivering light flashes across a high power field to optogenetically-evoked inhibitory currents (Figure 1D). We stimulated at 40 Hz to measure the ability of interneurons to generate synchronized  $\gamma$ -frequency inhibition (Figures 1E and 1F). The amplitudes of optogenetically-evoked IPSCs were much lower in *Dlx5/6*<sup>+/-</sup> mice (n = 16) compared to WT littermates (n = 14; p < 0.001). (To control for possible confounding differences in ChR2-eYFP expression, we confirmed that eYFP fluorescence was not decreased in *Dlx5/6*<sup>+/-</sup> mice; c.f. Figure S6C). Thus, in addition to the intrinsic abnormalities described above, there is an overall impairment in the ability of local inhibitory circuits to generate  $\gamma$ -frequency inhibition, and other interneuron subtypes do not simply compensate for FSIN deficits.

### ***Dlx5/6*<sup>+/-</sup> mice exhibit the post-adolescent onset of impaired cognitive flexibility**

Our next series of experiments examined whether these abnormalities in the post-adolescent development of FSINs and in local inhibitory output accompanied cognitive and behavioral endophenotypes of schizophrenia. We specifically assessed anxiety, cognitive flexibility, and social interaction. 7 week-old *Dlx5/6*<sup>+/-</sup> mice did not show significant differences in anxiety, measured by time spent in the center of a novel open field (n = 9 mice per genotype; Figure 2A) or the open arms of an elevated plus maze (EPM; WT, n = 4; *Dlx5/6*<sup>+/-</sup>, n = 5; Figure 2B). However, after 10 weeks of age, there was a significant increase in both measures of anxiety in *Dlx5/6*<sup>+/-</sup> mice compared to their WT littermates (open field: n = 9 WT and 8 *Dlx5/6*<sup>+/-</sup> mice, p < 0.01; EPM: n = 4 mice per genotype, p < 0.05; Figures 2A

and 2B). A similar age-dependent increase in anxiety was observed in *Dlx112b::Cre* × *Dlx5<sup>fl/-</sup>Dlx6<sup>+/-</sup>* mice (Figure S3A).

Next, we specifically assessed cognitive flexibility using a task (Figure 2C) in which a mouse learns to associate food reward with either an odor or a digging medium (initial association). In this task, mice are presented with two bowls on each trial, and must choose to dig in one bowl to find the food reward. Each bowl contains a different odor and a different digging medium, and the odor-medium combinations vary from trial to trial. Once the mouse has learned the initial association between food reward and a specific stimulus (either an odor or digging medium), the type of stimulus that predicts reward changes, e.g., from an odor to a digging medium or vice-versa, and the new rule must be learned (rule shift). As our data below shows, performance on this task depends strongly on the mPFC, and deficits in performance on this task observed in *Dlx5/6<sup>+/-</sup>* mice are stable across multiple days of testing.

At 7 weeks of age, both *Dlx5/6<sup>+/-</sup>* and WT mice (n = 5 per genotype) could learn the initial association and rule shift after similar numbers of trials (Figure 2D). However, after 10 weeks of age, while both groups of mice still learned the initial association in a similar number of trials, adult *Dlx5/6<sup>+/-</sup>* mice were specifically impaired during the rule-shifting portion of the task (n = 8 mice per genotype; p < 0.001; Figures 2F-2G). We further confirmed that adult *Dlx5/6<sup>+/-</sup>* mice had no deficiency in odor detection (Figure S3B). Finally, similar rule-shifting deficits occurred in *Dlx5/6<sup>+/-</sup>* mice backcrossed to CD1 for at least 6 generations, as well as in *Dlx112b::Cre* × *Dlx5<sup>fl/-</sup>Dlx6<sup>+/-</sup>* mice (Figures S3C-F).

We also tested whether *Dlx5/6<sup>+/-</sup>* mice could learn a new rule that was the reverse of the initial association. For example, if mice initially learned to associate an odor (garlic) with food reward, then the previously unrewarded odor (coriander) became associated with food reward. Initially, we simply appended this “rule reversal” to the end of our rule shift task (WT, n = 6; *Dlx5/6<sup>+/-</sup>*, n = 7; Figures 3A and 3B). We also carried out the rule reversal immediately following the initial association, then tested mice on a rule shift (n = 5; Figures 3A and 3C). In both cases, *Dlx5/6<sup>+/-</sup>* mice performed normally on the rule reversal, but were extremely impaired during the rule shift. This demonstrates that after *Dlx5/6<sup>+/-</sup>* mice form an initial association, they can learn a rule that is the reverse of that initial association, but not one based on a set of stimuli that were previously irrelevant to the outcome of each trial (Figure 3C). This broadly resembles the effects of mPFC lesions in a more extensive version of this task, in which mPFC lesions impair learning of associations based on previously irrelevant cues, but not the reversal of previously-learned associations (Bissonette et al., 2008). Furthermore, as we will describe, this selective impairment during rule shifts but not rule reversals is identical to the pattern elicited by acute optogenetic inhibition of mPFC interneurons.

In addition to measuring anxiety and cognitive flexibility, we also compared social interaction in *Dlx5/6<sup>+/-</sup>* and WT mice. We did not find differences in the time *Dlx5/6<sup>+/-</sup>* and WT mice spend investigating a novel juvenile mouse introduced into their home cage, although we did find differences in social interaction-induced EEG oscillations, described below.

## Adult *Dlx5/6*<sup>+/-</sup> mice exhibit increased baseline $\gamma$ oscillations and decreased task-evoked $\gamma$ oscillations

We implanted EEG electrodes at the dorsolateral border of PFC and recorded intracranial EEG from freely-moving mice of both genotypes at 7 weeks of age and in adults (at least 10 weeks old) (Figures 4A and 4B). First, we examined EEG power at baseline, when mice were resting in their home cage. Adult (n = 8 per genotype), but not 7 week old (n = 5 per genotype), *Dlx5/6*<sup>+/-</sup> mice exhibited an increase in baseline  $\gamma$  oscillations (Figures 4C and 4D). This is notable because whereas many studies of schizophrenia have reported decreases in  $\gamma$  oscillations evoked by tasks, others have reported increases in baseline or resting  $\gamma$  power (Lee et al., 2006; Mulert et al., 2010; Spencer et al., 2009). Elevations in baseline  $\gamma$  oscillations have also been observed in previous studies of mice with deficits in interneuron function (Carlen et al., 2012; Del Pino et al., 2013; Korotkova et al., 2010). We also verified that similar increases in baseline  $\gamma$  oscillations occur in *Dlx112b::Cre*  $\times$  *Dlx5*<sup>fl/-</sup> *Dlx6*<sup>+/-</sup> mice (Figure S4A).

Next, we examined whether in addition to *increased* baseline  $\gamma$  oscillations, we could also observe the *deficient* task-evoked  $\gamma$  oscillations that are associated with cognitive deficits in schizophrenia. For this, we recorded and analyzed prefrontal EEG activity during rule shifting. The recruitment of PFC  $\gamma$  oscillations by rule shifting was not markedly different in *Dlx5/6*<sup>+/-</sup> and WT mice at 7 weeks of age (Figure 4E), when *Dlx5/6*<sup>+/-</sup> mice perform normally. However, in adult *Dlx5/6*<sup>+/-</sup> mice, rule shifts recruited significantly less  $\gamma$  power (62-120 Hz) (Figure 4G). Thus, like the abnormalities in FSINs, anxiety, and cognitive flexibility described earlier, EEG abnormalities in *Dlx5/6*<sup>+/-</sup> mice only appear following adolescence. Notably, we confirmed that deficient rule shift-evoked  $\gamma$  oscillations are region specific, as EEG recordings over temporal cortex during rule shifting do not show  $\gamma$ -frequency differences between WT and *Dlx5/6*<sup>+/-</sup> mice (Figure S4C).

To test whether deficient  $\gamma$  oscillations could be observed during other PFC-dependent tasks, we recorded EEG activity during social interaction (Figures 4F and 4H). Notably, mPFC stimulation alters behavior during this task (Yizhar et al., 2011) and changes in mPFC activity also occur during social tasks in humans (Assaf et al., 2010). Task-evoked rhythmic activity was similar in *Dlx5/6*<sup>+/-</sup> and WT mice at 7 weeks of age (Figure 4F). By contrast, in adult mice, social interaction induced robust increases in PFC  $\gamma$  oscillations in WT, but not *Dlx5/6*<sup>+/-</sup> mice (Figure 4H). In fact, *Dlx5/6*<sup>+/-</sup> mice exhibited a slight decrease in prefrontal  $\gamma$  power. We observed similar deficits in *Dlx112b::Cre*  $\times$  *Dlx5*<sup>fl/-</sup> *Dlx6*<sup>+/-</sup> mice (Figure S4B). Thus, decreased task-evoked  $\gamma$  power, and increased baseline  $\gamma$  power both appear in *Dlx5/6*<sup>+/-</sup> mice in concert with the post-adolescent onset of FSIN abnormalities, suggesting that these phenomena may reflect a singular underlying pathological process.

## Optogenetically inhibiting mPFC interneurons specifically disrupts rule shifts but not rule reversals

To test whether mPFC interneuron dysfunction is sufficient to disrupt cognitive flexibility, we injected the mPFC of *Dlx112b-Cre* mice, which selectively express Cre in GABAergic interneurons (Han et al., 2012), with a Cre-dependent virus encoding the light-activated proton pump Archaeorhodopsin (Arch; Figure 5B). Controls consisted of *Dlx112b-Cre* mice

expressing eYFP or Cre-negative mice injected with AAV-DIO-Arch (throughout optogenetic experiments we were always blind about the identities of control mice). Once mice had learned the initial association, we delivered light to activate Arch bilaterally (530nm, 2.5 mW/side) throughout the rule shift portion of the task (Figures 5B and 5C). Arch-expressing mice (n = 5) were markedly impaired on the rule shift compared to Arch-negative controls (n = 4; Figures 5C and 5D), confirming that the rule shift depends on the mPFC, and specifically on mPFC interneurons.

To identify potential non-specific effects of inhibiting mPFC interneurons, we also activated Arch during initial associations or rule reversals. Neither initial association (n = 4 Arch-expressing mice and 3 controls; Figures S7D and S7E) nor rule reversal was affected by Arch activation compared to controls (n = 6 Arch-expressing mice and 5 controls; Figure 5E). This demonstrates that optogenetic inhibition of mPFC interneurons impairs the specific ability to learn a rule shift, but not nonspecific aspects of the task, learning of associations, or rule reversals. Thus, although optogenetically inhibiting mPFC interneurons is unlikely to completely mimic the consequences of chronic *Dlx5/6* deficiency, these results do establish that (1) selective rule shifting deficits can occur even when initial associations and rule reversals are normal, and (2) mPFC interneuron dysfunction is sufficient to explain the selective rule-shifting deficits observed in *Dlx5/6*<sup>+/-</sup> mice. The absence of an effect of mPFC interneuron inhibition on learning of a rule reversal following a successful rule shift may simply reflect the fact that our rule reversal does not depend on the mPFC, but may depend on mechanisms in the orbitofrontal cortex (Bissonette et al., 2008). Notably, we did not observe any seizures at the light power used for behavioral experiments.

### Enhancing GABAergic transmission rescues task-evoked $\gamma$ oscillations and cognitive flexibility in *Dlx5/6*<sup>+/-</sup> mice

The preceding results show that mPFC interneuron dysfunction is sufficient to disrupt rule shifts, and identify specific abnormalities in mPFC interneurons that we hypothesize drive schizophrenia-like deficits in task-evoked  $\gamma$  oscillations and cognitive flexibility in *Dlx5/6*<sup>+/-</sup> mice. If this hypothesis is correct, then enhancing inhibitory output may rescue these EEG and cognitive abnormalities. Enhancing GABAergic signaling with the benzodiazepine clonazepam (CLZ), a positive allosteric modulator of the GABA<sub>A</sub> receptor, treats social deficits in a mouse model of Dravet's syndrome (Han et al., 2012). Therefore, we tested the same low dose of CLZ (0.0625 mg kg<sup>-1</sup>) in *Dlx5/6*<sup>+/-</sup> mice. While this low dose did not exert sedative or anxiolytic effects on either WT or *Dlx5/6*<sup>+/-</sup> mice, CLZ completely normalized rule shifting in *Dlx5/6*<sup>+/-</sup> mice (n = 5 per genotype; Figures 6A-C).

CLZ also abolished differences in rule shift-evoked  $\gamma$  oscillations between *Dlx5/6*<sup>+/-</sup> and WT mice (n = 5 per genotype; Figure 6E). Note that we treated all mice with vehicle (VEH) on the day prior to CLZ treatment. On this day, mice performed the rule shift. Thus, in addition to comparing CLZ-treated *Dlx5/6*<sup>+/-</sup> mice to CLZ-treated WT mice, we could compare each *Dlx5/6*<sup>+/-</sup> mouse in the CLZ and VEH conditions. Indeed, we found that rule shifting evoked significantly stronger  $\gamma$  oscillations in *Dlx5/6*<sup>+/-</sup> mice during CLZ than during VEH treatment (n = 5 per condition; Figure 6D). Since rule shift-evoked  $\gamma$  oscillations were measured one day later in CLZ than in the VEH condition, this might

reflect an effect of training rather than of CLZ treatment. To rule out the possibility that training induces changes in  $\gamma$  oscillations between the first and second day of testing, we repeated rule shifting in a separate cohort of *Dlx5/6*<sup>+/-</sup> mice treated with VEH on two consecutive days (Figure S5A), and found no change in rule shifting evoked  $\gamma$  oscillations over the two days of VEH treatment (Figure S5B). Thus, CLZ treatment rescues both task-evoked  $\gamma$  oscillations and cognitive flexibility in *Dlx5/6*<sup>+/-</sup> mice. CLZ treatment also rescued cognitive flexibility in *Dlx112b::Cre*  $\times$  *Dlx5*<sup>fl/-</sup> *Dlx6*<sup>+/-</sup> mice (Figures S5C and S5D).

### **$\gamma$ -frequency optogenetic stimulation of mPFC interneurons normalizes cognitive flexibility in *Dlx5/6*<sup>+/-</sup> mice**

To test whether specifically inducing  $\gamma$ -frequency activity in mPFC interneurons could also enhance cognition, we injected mice with either the I12b-ChR2-eYFP virus described earlier, or a control I12b-mCherry virus, and implanted optical fibers in the mPFC bilaterally for optogenetic stimulation. We confirmed that the I12b-ChR2-eYFP virus specifically expresses ChR2 in GABAergic neurons, since all light-evoked synaptic currents were blocked by the GABAergic antagonists gabazine and CGP35348 (Figures S6A and S6B).

On Day 1, we assayed rule shifting in the absence of optogenetic stimulation in adult *Dlx5/6*<sup>+/-</sup> mice injected with either virus (Figure 7C and 7D). On Day 2, we repeated rule shifting while delivering optical stimulation at 40 Hz (470 nm, 5 msec pulses, ~0.25 mW/side). Even though 40 Hz is slightly lower than the frequency of rule-shift induced  $\gamma$  oscillations, we stimulated at this frequency because ChR2 stimulation around 40 Hz has previously been shown to be most effective for recruiting  $\gamma$  oscillations *in vivo* (Cardin et al., 2009) – higher frequencies may be less effective due to ChR2 kinetics. Once mice reached the criterion for learning the initial association, we began optogenetic stimulation, performed three additional trials of the initial association, and then began the rule shift. Stimulation continued throughout the rule shift. On Day 3, we repeated the initial association and rule shift tasks again, in the absence of optogenetic stimulation.

As expected, both ChR2 and mCherry-expressing mice took an abnormally large number of trials to learn the rule shift on Day 1. However, on Day 2, optogenetic stimulation completely normalized rule shifting in ChR2-expressing mice (ChR2, n = 7; mCherry, n = 4; Figure 7D). Remarkably, on Day 3 of rule shifting, the ChR2-expressing mice continued to perform normally, whereas rule-shifting deficits persisted in mCherry-expressing mice (ChR2, n = 6; mCherry, n = 4; Figures 7D and 7E).

We also made prefrontal EEG recordings from both mCherry and ChR2-expressing *Dlx5/6*<sup>+/-</sup> mice as they performed the rule shift task in the presence or absence of 40 Hz optogenetic stimulation. In ChR2-expressing *Dlx5/6*<sup>+/-</sup> mice, optogenetic stimulation dramatically increased power at 40 Hz (Figure 7B), and this peak was absent in mCherry-expressing mice (Figure 7A). Interestingly, this increase in  $\gamma$  did not persist on Day 3 of testing, when mice no longer receive stimulation but continue to perform normally (see Discussion). Finally, we also rescued rule-shifting in ChR2-expressing *Dlx5/6*<sup>+/-</sup> mice using 60 Hz optogenetic stimulation (470 nm, 3.3 msec pulses, ~0.25mW/side; ChR2, n = 4; mCherry, n = 3; Figures 7I-K).



## Pro-cognitive effects of stimulating mPFC interneurons are frequency-specific and long-lasting

To test whether the ability of optogenetic stimulation to rescue rule shifting is frequency-specific, we assayed rule shifting in the absence of optogenetic stimulation on Day 1 (Figures 7F and 7G). Then, on Day 2, we delivered optogenetic stimulation using a combination of frequencies above and below the  $\gamma$  band. Specifically, we delivered bursts of 4 msec light flashes with an *inter*-burst frequency of 12.5 Hz, an *intra*-burst frequency of 125 Hz, and 4 flashes / burst. Thus, the total amount of light stimulation using this protocol (denoted for simplicity as “12.5 Hz”) was the same as in our 40 or 60 Hz stimulation protocol (200 msec / second). This 12.5 Hz protocol loosely resembles theta burst stimulation, and was selected to employ an interburst frequency well outside the  $\gamma$  range, along with bursts of flashes (instead of long continuous light pulses) to minimize ChR2 inactivation. On Day 3, we delivered 40 Hz optogenetic stimulation. Again, we injected *Dlx5/6*<sup>+/-</sup> mice bilaterally with either the I12b-ChR2-eYFP virus, or a control I12b-mCherry virus (n = 5 per condition). On Day 2, the 12.5 Hz optogenetic stimulation did not improve rule shifting. In fact, 12.5 Hz stimulation caused a non-significant *increase* in both the number of trials required for learning and errors (Figures 7G and 7H) in ChR2-expressing mice. By contrast, on Day 3, 40 Hz stimulation again completely normalized rule-shifting. We waited one week, and then tested both ChR2-expressing and control mice again in the absence of additional light stimulation on Day 10. Surprisingly, the mice that had received 40 Hz optogenetic stimulation continued to exhibit markedly-improved rule shifting one week later (Figures 7G and 7H).

Finally, we delivered 12.5 or 40 Hz stimulation to wild-type mice that had been injected with AAV-I12b-ChR2-eYFP and measured their performance during the rule shift task. Neither pattern of stimulation altered performance (Figures S7A-C). This lack of effect is consistent with the relatively low light power used for stimulation, and suggests that these are weak patterns of optogenetic stimulation which serve to perturb, rather than radically alter, PFC activity.

## DISCUSSION

We have demonstrated that the post-adolescent appearance of deficits in FSIN function accompanies the onset of behavioral, cognitive, and EEG endophenotypes of schizophrenia in *Dlx5/6*<sup>+/-</sup> mice. Furthermore, inhibiting mPFC interneurons in wild-type mice is sufficient to recapitulate the specific deficit in rule shifting observed in *Dlx5/6*<sup>+/-</sup> mice. Conversely, impaired cognitive flexibility in *Dlx5/6*<sup>+/-</sup> mice can be rescued either by globally-enhancing inhibitory synaptic output with CLZ, or by selectively-stimulating mPFC interneurons at  $\gamma$  frequency. Strikingly, the pro-cognitive effects of interneuron stimulation are specific to  $\gamma$ -frequency stimulation at 40 or 60 Hz, and do not generalize to stimulation using a combination of higher and lower frequencies. Moreover, following 40 Hz stimulation, mice continue to perform rule shifting normally one week later, even in the absence of additional optogenetic stimulation. These results demonstrate how disruptions in factors which direct the development of MGE-derived interneurons can, as hypothesized (Volk and Lewis, 2013), elicit key aspects of schizophrenia including prominent deficits in

FSINs,  $\gamma$  oscillations, and PFC-dependent cognition. Our studies also illustrate a specific mechanism – the abnormal post-adolescent development of FSINs – that may contribute to the post-adolescent emergence of cognitive deficits and abnormal  $\gamma$  oscillations in schizophrenia. Most strikingly, our results firmly establish that  $\gamma$ -frequency activity within prefrontal interneurons can, as has long been hypothesized, powerfully influence cognitive domains at the core of schizophrenia.

### **Cognitive deficits in *Dlx5/6*<sup>+/-</sup> mice are specific and persistent, and model a key endophenotype of schizophrenia**

Each day, mice learn flexible associations between stimuli and food rewards. Then, at the end of each day, we filled bowls with different odor-medium combinations, distributed food equally among these bowls, and presented them to mice so as to eliminate that day's stimulus-food associations. As a result, when we repeated this task across multiple days, ChR2-negative *Dlx5/6*<sup>+/-</sup> mice were consistently and selectively impaired during the rule shift but not the initial association (cf. mCherry-expressing mice in Figures 7D-H and Figures S6D and S6E). Similarly, *Dlx5/6*<sup>+/-</sup> mice (and mice in which we optogenetically inhibit mPFC interneurons) were impaired on rule shifts but not rule reversals. These results clearly establish that our rule-shifting task measures a specific aspect of cognitive flexibility that is strongly dependent on prefrontal interneurons and persistently impaired in *Dlx5/6*<sup>+/-</sup> mice. Interestingly, rule reversals, which are believed to depend on OFC, are not impaired in *Dlx5/6*<sup>+/-</sup> mice, suggesting either that OFC-mediated reversal learning is less dependent on FSINs, or that FSINs are less impaired within the OFC of *Dlx5/6*<sup>+/-</sup> mice.

### **Restoring interneuron-driven $\gamma$ oscillations induces persistent pro-cognitive effects**

Remarkably, optogenetic stimulation can overcome this otherwise fixed cognitive deficit we found in *Dlx5/6*<sup>+/-</sup> mice and induce persistent improvements in their cognitive flexibility. While the persistent nature of this cognitive rescue may seem surprising, it is consistent with studies showing that effective learning can overcome rule-shifting deficits associated with schizophrenia in human subjects. In one study (Krystal et al., 2000), volunteers performed the Wisconsin Card Sorting Task (WCST) after receiving ketamine on one day, and saline on another. Ketamine induces cognitive deficits similar to schizophrenia, and volunteers who received ketamine on the first day were extremely impaired on the WCST. By contrast, volunteers who received saline on the first day performed normally when they subsequently received ketamine. In the second study, many subjects with schizophrenia who receive explicit instructions about the WCST improve to near normal levels of performance after just one training session (Pedersen et al., 2012). These studies suggest that once a subject understands the WCST, then that individual is able to perform the task normally, even in the presence of either schizophrenia itself, or ketamine-induced cognitive deficits which model schizophrenia. This parallels the situation in our study: we rescue cognitive deficits using optogenetic stimulation, allowing *Dlx5/6*<sup>+/-</sup> mice to learn the rule shift efficiently. Having experienced effective learning during one rule shift, *Dlx5/6*<sup>+/-</sup> mice subsequently perform normally when tested again in the absence of optogenetic stimulation. In particular, the persistent nature of the improvements in cognition we observed following  $\gamma$ -frequency stimulation suggests that acutely restoring interneuron-driven rhythms during cognitive

training might potentiate learning in a way that could enhance cognitive remediation in schizophrenia (Subramaniam et al., 2012).

Interestingly, improved performance one day after optogenetic stimulation in *Dlx5/6<sup>+/-</sup>* mice was not associated with persistently-enhanced  $\gamma$  oscillations. This suggests that  $\gamma$ -frequency stimulation does not chronically enhance the ability of prefrontal inhibitory circuits to generate  $\gamma$  oscillations, but rather, may establish a representation of the task, either in the PFC and/or in downstream structures (e.g., striatum), that facilitates subsequent rule shifts even in the absence of “normal” task-evoked  $\gamma$  oscillations.

Although cortical  $\gamma$  oscillations have been hypothesized to contribute to cognition for decades (Gray and Singer, 1989; Llinas et al., 1991; Rodriguez et al., 1999; Salinas and Sejnowski, 2001), this is, to our knowledge, the first causal and specific demonstration that cortical  $\gamma$  oscillations can exert pro-cognitive effects in behaving mice. This builds on previous work showing that optogenetic activation of PV interneurons at  $\gamma$  frequencies can enhance the precision of spikes and information coding in single neurons (Cardin et al., 2009; Sohal et al., 2009). A more recent study showed that stimulating PV interneurons in S1 at  $\gamma$  frequency can enhance the detection of less salient tactile stimuli (Siegle et al., 2014), and this may relate to an earlier finding that nonspecifically activating PV interneurons sharpens orientation turning in V1 and enhances orientation discrimination by behaving mice (Lee et al., 2012). Together with those studies, our results suggest that interneuron-driven  $\gamma$  oscillations can enhance neural information processing across a broad range of scales and contexts, ranging from signal detection by single neurons or neuronal populations within primary sensory cortex, to association cortices performing more abstract computations.

It will be important for future studies to elucidate details about the process through which interneuron-driven  $\gamma$  oscillations can enhance cognition. Notably, 40 Hz stimulation could rescue rule shifting even though this frequency is slightly lower than that of actual rule shifting-induced  $\gamma$  oscillations. This suggests that 40 Hz oscillations (but not 12.5 Hz oscillations) can effectively supplant slightly higher frequency  $\gamma$  activity. In addition, while 40 or 60 Hz stimulation is clearly effective whereas 12.5 Hz stimulation is not, it is unclear what mechanism accounts for this specificity. In particular, it is possible that the pro-cognitive effects of 40 or 60 Hz stimulation reflect the fact that these frequencies are particularly effective at recruiting FSIN output and entraining the local circuit (Cardin et al., 2009). Alternatively, there may be something particularly advantageous about entraining the local circuit at 40 or 60 Hz compared to other frequencies. Regardless, our results clearly demonstrate that  $\gamma$ -frequency activation of PFC interneurons is particularly efficacious for restoring cognition.

Although our results clearly link PFC interneuron-driven  $\gamma$  oscillations with cognitive flexibility, the precise cellular defects that cause deficient task-evoked  $\gamma$  oscillations in *Dlx5/6<sup>+/-</sup>* mice remain unclear. While FSINs are known to play major roles in  $\gamma$  oscillations, and we observed intrinsic deficits in FSINs but not in non-FS interneurons or pyramidal neurons (c.f. Figures S2A and S2B), we cannot exclude the possibility that other classes of interneurons contribute to cognitive inflexibility and/or deficient task-evoked  $\gamma$  oscillations

in *Dlx5/6<sup>+/-</sup>* mice. Indeed, other classes of interneurons exhibit less prominent abnormalities in schizophrenia (Volk and Lewis, 2013). On a finer scale, beyond finding diminished IPSCs evoked by  $\gamma$ -frequency stimulation of PFC interneurons, we have not worked out the details of how abnormal FSIN intrinsic properties “add up,” together with possible deficiencies in FSIN input and output, to cause a net effect such as FSIN dysfunction. That being said, *Dlx5/6<sup>+/-</sup>* mice exhibit the prominent FSIN abnormalities, abnormal  $\gamma$  oscillations, and cognitive inflexibility characteristic of schizophrenia, and thus represent a useful system for evaluating the relationship between interneuron-driven  $\gamma$  oscillations and cognitive endophenotypes. We have focused on cognitive flexibility, but future studies should explore how PFC interneuron-driven  $\gamma$  oscillations might contribute to other behaviors, e.g., anxiety or social interaction (for which we observed abnormal  $\gamma$  oscillations but no change in behavior).

Low dose CLZ also restored prefrontal task-evoked  $\gamma$  oscillations and rescued cognitive flexibility in *Dlx5/6<sup>+/-</sup>* mice. While benzodiazepines are used to treat anxiety and agitation in schizophrenia, the cognitive effects of augmenting GABAergic function have been less well studied with mixed results (Lewis et al., 2008). As in a previous study which used CLZ to rescue social deficits in a mouse model of Dravet's syndrome (Han et al., 2012), the low dose of CLZ we used may have been particularly important for its therapeutic effects by minimizing sedation and/or maximizing the relative selectivity of CLZ for  $\alpha 2$  or  $\alpha 3$  subunit-containing GABA<sub>A</sub> receptors, which have been proposed to exert pro-cognitive effects in schizophrenia (Lewis et al., 2008).

Several observations argue against the idea that ongoing seizure activity contributes to cognitive deficits in *Dlx5/6<sup>+/-</sup>* mice. First, we never observed behavioral or electrographic seizures in awake, behaving *Dlx5/6<sup>+/-</sup>* mice. Indeed, a previous study of *Dlx5/6<sup>+/-</sup>* mice found a total of just 32 seconds of seizure activity spread across 34 days of EEG recording (Wang et al., 2010). Second, it would be remarkable if seizures could selectively impair learning during rule shifts, but not during initial associations or rule reversals. Finally, even low frequencies of interneuron stimulation should strongly suppress seizures. Thus, the fact that only 40 or 60 Hz stimulation rescues cognition, suggests that this cognitive rescue does not reflect an anticonvulsant mechanism.

## Conclusions

In summary, our studies provide critical evidence for long-hypothesized relationships between interneurons,  $\gamma$  oscillations, and PFC-dependent cognition. They also illustrate how the abnormal development of FSINs might disrupt  $\gamma$  oscillations and thereby drive the post-adolescent onset of aspects of schizophrenia. Future studies that elucidate the detailed process of interneuron development, including molecular pathways connecting *Dlx5/6* to FSIN development, may thus further advance our understanding of the pathophysiology of schizophrenia and related conditions, while interventions that acutely enhance interneuron-driven  $\gamma$  rhythms may represent new avenues for treatment.

## EXPERIMENTAL PROCEDURES

A brief summary is provided here, with more detail in the Supplemental Information accompanying this article.

All experiments were conducted in accordance with procedures established by the Administrative Panels on Laboratory Animal Care at the University of California, San Francisco. *Dlx5/6*<sup>+/-</sup> mice were generated as previously described (Wang et al., 2010), and maintained on either a CD1 or a mixed CD1 and C57Bl/6 background. Unless otherwise noted, subjects were fed *ad libitum* and reared in normal lighting conditions (12/12 light/dark cycle).

Electrophysiological recordings used mice of both genders at three ages: juvenile (P16-20), adolescent (P45-49), and adult (P63-88). Behavioral analyses used male mice that were adolescents (P46-52) or adults (P70-121), except the experiment using optogenetic inhibition during an initial association, which used adult female *H2b-Cre* mice. For some behavioral experiments, animals were implanted with EEG recording electrodes. After allowing animals to recover from surgery, we recorded differential EEG at 1 kHz using a time-locked video EEG monitoring system (Pinnacle Technology). In other cases, prior to behavioral experiments, animals were injected with AAV to drive expression of *H2b-ChR2-eYFP*, *H2b-mCherry*, *DIO-Arch3.0-eYFP*, or *DIO-eYFP*, and implanted with dual fiberoptic cannulae (Doric Lenses, Inc.) for optogenetic stimulation. For details about electrophysiology, immunohistochemistry, EEG surgeries, virus injections and implantations, and optogenetic stimulation, see the Supplemental Experimental Procedures.

The open-field, elevated plus maze, social interaction, and cognitive flexibility testing in mice are described in the Supplemental Experimental Procedures along with additional details and discussion of the behavioral training, recordings, and data analyses.

Data was analyzed using custom software written in Matlab (The MathWorks, Natick, MA). In general, two-tailed Student's t-tests were used to compare pairs of groups, unless there were repeated measurements or >2 groups in which case ANOVA was used. Error bars indicate  $\pm 1$  SEM unless otherwise specified. All statistical tests are described in detail in Supplemental Experimental Procedures.

## Supplementary Material

Refer to Web version on PubMed Central for supplementary material.

## ACKNOWLEDGEMENTS

We are grateful to Ramón Pla Ferriz for his assistance with breeding and genotyping mice. We thank Nigel Killeen and the UCSF ES cell core for making the floxed *Dlx5* allele. This work was supported by the Staglin Family and International Mental Health Research Organization, NIMH (R00MH085946 and R01MH100292), the Alfred P. Sloan Foundation, and the NIH Office of the Director (DP2MH100011), a NIH training grant to KKAC (T32MH89920), and the Brain and Behavior Foundation (NARSAD Young Investigator Award to KKAC). JLRR is supported by NIMH (R37MH049428).

## REFERENCES

- Assaf M, Jagannathan K, Calhoun VD, Miller L, Stevens MC, Sahl R, O'Boyle JG, Schultz RT, Pearlson GD. Abnormal functional connectivity of default mode sub-networks in autism spectrum disorder patients. *Neuroimage*. 2010; 53:247–256. [PubMed: 20621638]
- Belforte JE, Zsiros V, Sklar ER, Jiang Z, Yu G, Li Y, Quinlan EM, Nakazawa K. Postnatal NMDA receptor ablation in corticolimbic interneurons confers schizophrenia-like phenotypes. *Nature neuroscience*. 2010; 13:76–83. [PubMed: 19915563]
- Bissonette GB, Martins GJ, Franz TM, Harper ES, Schoenbaum G, Powell EM. Double dissociation of the effects of medial and orbital prefrontal cortical lesions on attentional and affective shifts in mice. *J Neurosci*. 2008; 28:11124–11130. [PubMed: 18971455]
- Bissonette GB, Schoenbaum G, Roesch MR, Powell EM. Interneurons Are Necessary for Coordinated Activity During Reversal Learning in Orbitofrontal Cortex. *Biological psychiatry*. 2014
- Cardin JA, Carlen M, Meletis K, Knoblich U, Zhang F, Deisseroth K, Tsai LH, Moore CI. Driving fast-spiking cells induces gamma rhythm and controls sensory responses. *Nature*. 2009; 459:663–667. [PubMed: 19396156]
- Carlen M, Meletis K, Siegle JH, Cardin JA, Futai K, Vierling-Claassen D, Ruhlmann C, Jones SR, Deisseroth K, Sheng M, et al. A critical role for NMDA receptors in parvalbumin interneurons for gamma rhythm induction and behavior. *Molecular psychiatry*. 2012; 17:537–548. [PubMed: 21468034]
- Cauli B, Audinat E, Lambolez B, Angulo MC, Ropert N, Tsuzuki K, Hestrin S, Rossier J. Molecular and physiological diversity of cortical nonpyramidal cells. *J Neurosci*. 1997; 17:3894–3906. [PubMed: 9133407]
- Cho RY, Konecky RO, Carter CS. Impairments in frontal cortical gamma synchrony and cognitive control in schizophrenia. *Proc Natl Acad Sci U S A*. 2006; 103:19878–19883. [PubMed: 17170134]
- Del Pino I, Garcia-Frigola C, Dehorter N, Brotons-Mas JR, Alvarez-Salvado E, Martinez de Lagran M, Ciceri G, Gabaldon MV, Moratal D, Dierssen M, et al. Erbb4 Deletion from Fast-Spiking Interneurons Causes Schizophrenia-like Phenotypes. *Neuron*. 2013; 79:1152–1168. [PubMed: 24050403]
- Goldberg EM, Jeong HY, Kruglikov I, Tremblay R, Lazarenko RM, Rudy B. Rapid developmental maturation of neocortical FS cell intrinsic excitability. *Cerebral cortex*. 2011; 21:666–682. [PubMed: 20705896]
- Gray CM, Singer W. Stimulus-specific neuronal oscillations in orientation columns of cat visual cortex. *Proc Natl Acad Sci U S A*. 1989; 86:1698–1702. [PubMed: 2922407]
- Green MF. Cognitive impairment and functional outcome in schizophrenia and bipolar disorder. *J Clin Psychiatry*. 2006; 67:e12. [PubMed: 17107235]
- Han S, Tai C, Westenbroek RE, Yu FH, Cheah CS, Potter GB, Rubenstein JL, Scheuer T, de la Iglesia HO, Catterall WA. Autistic-like behaviour in *Scn1a*<sup>+/-</sup> mice and rescue by enhanced GABA-mediated neurotransmission. *Nature*. 2012; 489:385–390. [PubMed: 22914087]
- Kawaguchi Y, Kubota Y. Correlation of physiological subgroupings of nonpyramidal cells with parvalbumin- and calbindinD28k-immunoreactive neurons in layer V of rat frontal cortex. *Journal of neurophysiology*. 1993; 70:387–396. [PubMed: 8395585]
- Korotkova T, Fuchs EC, Ponomarenko A, von Engelhardt J, Monyer H. NMDA receptor ablation on parvalbumin-positive interneurons impairs hippocampal synchrony, spatial representations, and working memory. *Neuron*. 2010; 68:557–569. [PubMed: 21040854]
- Krystal JH, Bennett A, Abi-Saab D, Belger A, Karper LP, D'Souza DC, Lipschitz D, Abi-Dargham A, Charney DS. Dissociation of ketamine effects on rule acquisition and rule implementation: possible relevance to NMDA receptor contributions to executive cognitive functions. *Biol Psychiatry*. 2000; 47:137–143. [PubMed: 10664830]
- Lee AT, Gee SM, Vogt D, Patel T, Rubenstein JL, Sohal VS. Pyramidal neurons in prefrontal cortex receive subtype-specific forms of excitation and inhibition. *Neuron*. 2014; 81:61–68. [PubMed: 24361076]

- Lee S-H, Wynn JK, Green MF, Kim H, Lee K-J, Nam M, Park J-K, Chung Y-C. Quantitative EEG and low resolution electromagnetic tomography (LORETA) imaging of patients with persistent auditory hallucinations. *Schizophrenia research*. 2006; 83:111–119. [PubMed: 16524699]
- Lee SH, Kwan AC, Zhang S, Phoumthippavong V, Flannery JG, Masmanidis SC, Taniguchi H, Huang ZJ, Zhang F, Boyden ES, et al. Activation of specific interneurons improves V1 feature selectivity and visual perception. *Nature*. 2012; 488:379–383. [PubMed: 22878719]
- Lewis DA, Cho RY, Carter CS, Eklund K, Forster S, Kelly MA, Montrose D. Subunit-selective modulation of GABA type A receptor neurotransmission and cognition in schizophrenia. *Am J Psychiatry*. 2008; 165:1585–1593. [PubMed: 18923067]
- Lewis DA, Hashimoto T, Volk DW. Cortical inhibitory neurons and schizophrenia. *Nat Rev Neurosci*. 2005; 6:312–324. [PubMed: 15803162]
- Llinas RR, Grace AA, Yarom Y. In vitro neurons in mammalian cortical layer 4 exhibit intrinsic oscillatory activity in the 10- to 50-Hz frequency range. *Proc Natl Acad Sci U S A*. 1991; 88:897–901. [PubMed: 1992481]
- Minzenberg MJ, Carter CS. Developing treatments for impaired cognition in schizophrenia. *Trends Cogn Sci*. 2012; 16:35–42. [PubMed: 22178120]
- Minzenberg MJ, Firl AJ, Yoon JH, Gomes GC, Reinking C, Carter CS. Gamma Oscillatory Power is Impaired During Cognitive Control Independent of Medication Status in First-Episode Schizophrenia. *Neuropsychopharmacology : official publication of the American College of Neuropsychopharmacology*. 2010
- Mulert C, Kirsch V, Pascual-Marqui R, McCarley RW, Spencer KM. Long- range synchrony of gamma oscillations and auditory hallucination symptoms in schizophrenia. *International journal of psychophysiology : official journal of the International Organization of Psychophysiology*. 2010
- Okaty BW, Miller MN, Sugino K, Hempel CM, Nelson SB. Transcriptional and electrophysiological maturation of neocortical fast-spiking GABAergic interneurons. *J Neurosci*. 2009; 29:7040–7052. [PubMed: 19474331]
- Pedersen A, Wilmsmeier A, Wiedl KH, Bauer J, Kueppers K, Koelkebeck K, Kohl W, Kugel H, Arolt V, Ohrmann P. Anterior cingulate cortex activation is related to learning potential on the WCST in schizophrenia patients. *Brain Cogn*. 2012; 79:245–251. [PubMed: 22554566]
- Penttonen M, Kamondi A, Acsády L, Buzsáki G. Gamma frequency oscillation in the hippocampus of the rat: intracellular analysis in vivo. *The European journal of neuroscience*. 1998; 10:718–728. [PubMed: 9749733]
- Rodriguez E, George N, Lachaux JP, Martinerie J, Renault B, Varela FJ. Perception's shadow: long-distance synchronization of human brain activity. *Nature*. 1999; 397:430–433. [PubMed: 9989408]
- Salinas E, Sejnowski TJ. Correlated neuronal activity and the flow of neural information. *Nat Rev Neurosci*. 2001; 2:539–550. [PubMed: 11483997]
- Saunders JA, Gandal MJ, Siegel SJ. NMDA antagonists recreate signal-to-noise ratio and timing perturbations present in schizophrenia. *Neurobiol Dis*. 2012; 46:93–100. [PubMed: 22245663]
- Siegle JH, Pritchett DL, Moore CI. Gamma-range synchronization of fast-spiking interneurons can enhance detection of tactile stimuli. *Nature neuroscience*. 2014; 17:1371–1379. [PubMed: 25151266]
- Sohal VS, Zhang F, Yizhar O, Deisseroth K. Parvalbumin neurons and gamma rhythms enhance cortical circuit performance. *Nature*. 2009; 459:698–702. [PubMed: 19396159]
- Spencer KM, Niznikiewicz MA, Nestor PG, Shenton ME, McCarley RW. Left auditory cortex gamma synchronization and auditory hallucination symptoms in schizophrenia. *BMC neuroscience*. 2009; 10:85–85. [PubMed: 19619324]
- Subramaniam K, Luks T, Fisher M, Simpson G, Nagarajan S, Vinogradov S. Computerized Cognitive Training Restores Neural Activity within the Reality Monitoring Network in Schizophrenia. *Neuron*. 2012; 73:842–853. [PubMed: 22365555]
- Uhlhaas PJ, Singer W. Abnormal neural oscillations and synchrony in schizophrenia. *Nature reviews Neuroscience*. 2010; 11:100–113. [PubMed: 20087360]
- Volk DW, Lewis DA. Prenatal ontogeny as a susceptibility period for cortical GABA neuron disturbances in schizophrenia. *Neuroscience*. 2013; 248C:154–164. [PubMed: 23769891]

- Wang Y, Dye CA, Sohal V, Long JE, Estrada RC, Roztocil T, Lufkin T, Deisseroth K, Baraban SC, Rubenstein JL. Dlx5 and Dlx6 regulate the development of parvalbumin-expressing cortical interneurons. *J Neurosci*. 2010; 30:5334–5345. [PubMed: 20392955]
- Yizhar O, Fenno LE, Prigge M, Schneider F, Davidson TJ, O'Shea DJ, Sohal VS, Goshen I, Finkelstein J, Paz JT, et al. Neocortical excitation/inhibition balance in information processing and social dysfunction. *Nature*. 2011; 477:171–178. [PubMed: 21796121]



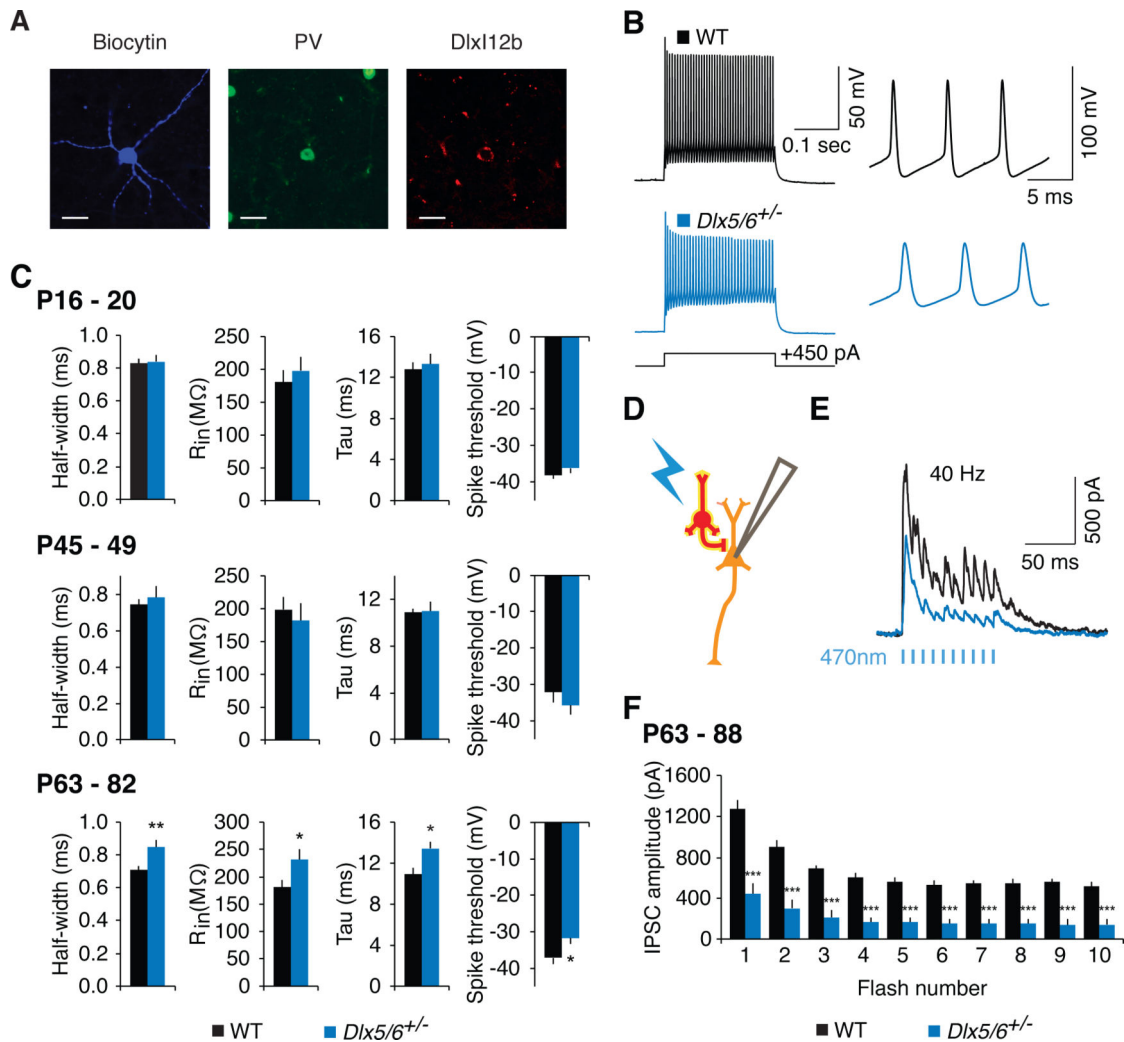


**Figure 1. Intrinsic properties of fast-spiking parvalbumin (PV) interneurons become abnormal following adolescence in *Dlx5/6*<sup>+/-</sup> mice**

(A) A fast-spiking interneuron (FSIN) in layer 5 of adult (P71) mouse prefrontal cortex that was filled with biocytin (blue) and later confirmed to express PV (green); scale bar = 20 μm. Putative interneurons were initially identified by the expression of AAV-Dlx12b-mCherry (red).

(B) Example current-clamp responses of adult FSINs to injection of depolarizing current in wild-type (black) and *Dlx5/6*<sup>+/-</sup> (blue) mice.

(C) The action potential half-width, input resistance, membrane time constant, and action potential threshold, calculated from current clamp responses of P16-P20 (juvenile), P45-49 (adolescent), and P63-82 (adult) FSINs to brief current pulses (-50 pA for input resistance, 100 pA above spiking threshold for other parameters).

(D) Whole-cell recordings were made from layer 5 pyramidal neurons (orange) in prefrontal brain slices from P63-88 mice, while stimulating ChR2 (yellow) in *Dlx12b*-expressing interneurons (red). Pyramidal neurons were voltage clamped at +10 mV.

(E) Example inhibitory currents recorded from layer 5 pyramidal neurons in response to 40 Hz interneuron stimulation in WT (black) and *Dlx5/6*<sup>+/-</sup> (blue) mice.

(F) Population average of the IPSC amplitudes evoked by 40 Hz optogenetic stimulation of interneurons.

All data show means  $\pm$  SEM. \* $p < 0.05$ , \*\* $p < 0.01$ , \*\*\* $p < 0.001$ .

See also Figures S1, S2.

Author Manuscript

Author Manuscript

Author Manuscript

Author Manuscript

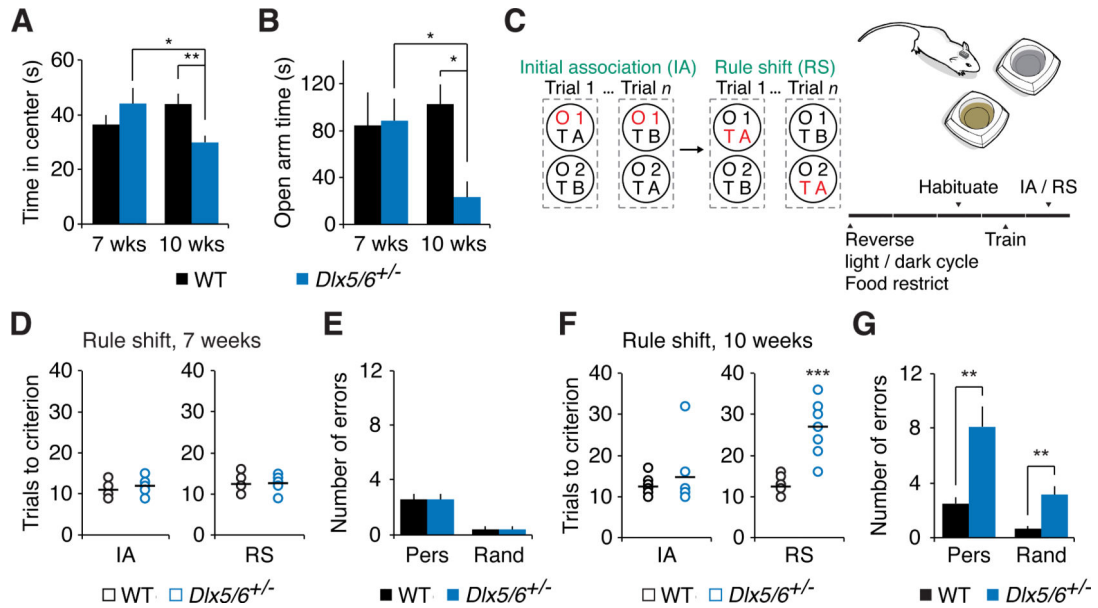


**Figure 2. *Dlx5/6*<sup>+/-</sup> mice exhibit a post-adolescent onset of increased anxiety and impaired cognitive flexibility**

(A) 7 week old *Dlx5/6*<sup>+/-</sup> mice and their WT littermates spend similar amounts of time in the center of an open field. In a distinct 10 week old cohort, *Dlx5/6*<sup>+/-</sup> mice spend less time in the center than do WT littermates.

(B) In the elevated plus maze, 7 week old *Dlx5/6*<sup>+/-</sup> mice and their WT littermates spend similar amounts of time in the open arms. In a distinct 10 week old cohort, *Dlx5/6*<sup>+/-</sup> mice spend less time in the open arms than do WT littermates.

(C) Schematic illustrating the rule-shifting task, in which mice chose one of two bowls, each baited by an odor (O1 or O2) and a textured digging medium (TA or TB), to find a food reward (the stimulus associated with reward is indicated in red). Mice first learn an initial association (IA) between a stimulus (e.g., odor O1) and food reward. Once mice reach the learning criterion (8 correct out of 10 consecutive trials), this association undergoes an extra-dimensional rule shift (RS), e.g., from O1 to a texture (TA). Mice adapt to a reversed light/dark cycle, undergo food restriction, and are habituated to the bowls, textured digging media, and food rewards before beginning testing.

(D) Performance in the initial association and rule-shift is similar for 7 week old *Dlx5/6*<sup>+/-</sup> and WT mice.

(E) There is no significant difference in “perseverative” errors, i.e., errors that are consistent with the initial rule, for 7 week old *Dlx5/6*<sup>+/-</sup> and WT mice.

(F) Performance of adult *Dlx5/6*<sup>+/-</sup> mice and their WT littermates on the initial association and rule shift.

(G) During the rule-shift, *Dlx5/6*<sup>+/-</sup> mice made a preponderance of perseverative errors compared to “random errors,” i.e., errors that are inconsistent with both the old and new rules.

All data show means ± SEM and analyzed using two-tailed Student's unpaired t-tests. \*p < 0.05, \*\*p < 0.01, \*\*\*p < 0.001.

See also Figure S3.

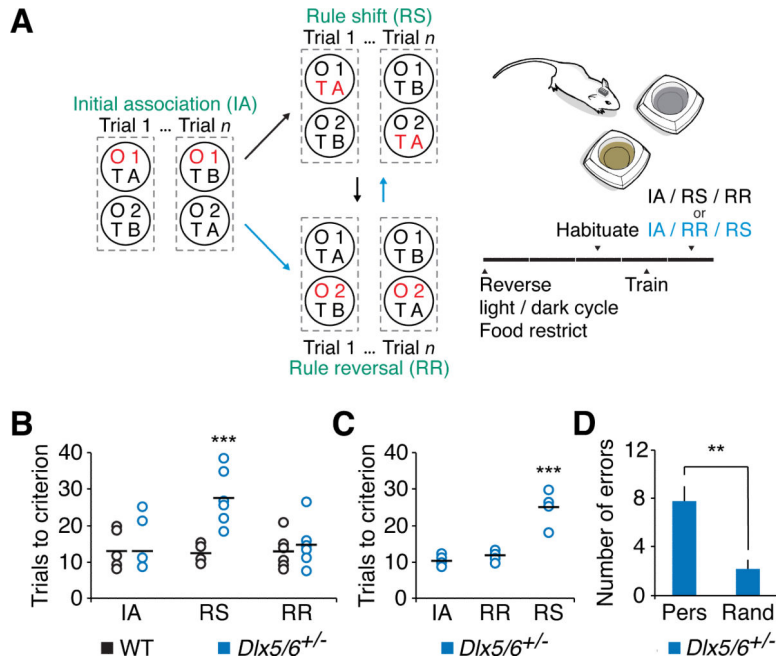


**Figure 3. *Dlx5/6*<sup>+/-</sup> mice are not impaired in rule reversals**

(A) Schematic illustrating how we assayed rule reversals either before or after rule shifts. In all cases, mice first learn an initial association between the food reward and one stimulus, e.g., odor 1 (O1). In some cases (black arrows), the mice then experience a rule shift (RS) in which a previously irrelevant stimulus, e.g., texture A (TA), becomes associated with reward. In the other cases (blue arrows), immediately following the initial association, mice learn a rule reversal (RR), in which the stimulus that was unrewarded during the initial association, e.g., odor 2 (O2), now becomes associated with reward. In both cases, all three portions of the task (IA / RS / RR or IA / RR / RS) were completed consecutively on one day. The rule reversal always tested the ability of mice to learn a reversal of the association that they had successfully acquired during the IA, whereas the rule shift always tested mice on their ability to learn a rule based a stimulus that was previously irrelevant to the outcome of each trial.

(B) Performance of adult *Dlx5/6*<sup>+/-</sup> mice and their wild-type littermates in the IA, followed by the RS, and RR.

(C) Performance of adult *Dlx5/6*<sup>+/-</sup> mice in the IA, followed by the RR, and RS.

(D) During the rule shift shown in (C), adult *Dlx5/6*<sup>+/-</sup> mice made a preponderance of perseverative errors, compared to random errors.

All data show means ± SEM and are analyzed using two-tailed Student's t-tests. \*\*p < 0.01, \*\*\*p < 0.001.

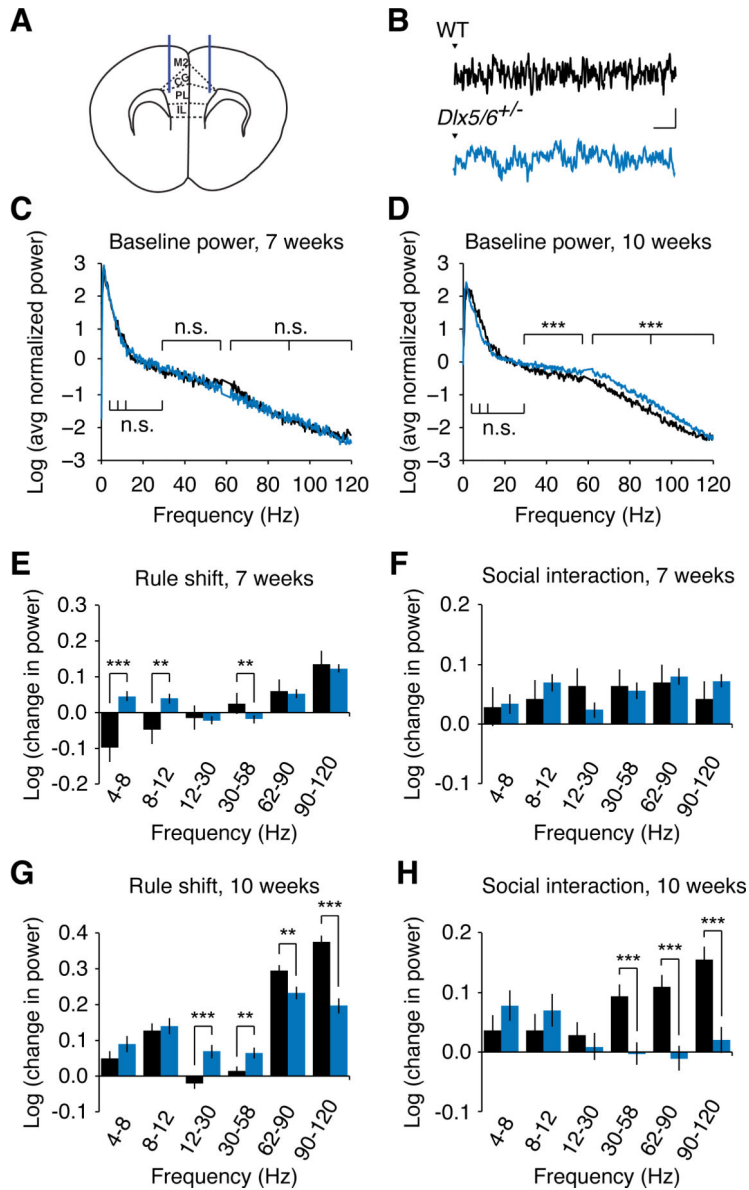


**Figure 4. Adult (but not adolescent) *Dlx5/6<sup>+/-</sup>* mice exhibit abnormal baseline  $\gamma$  oscillations and deficient task-evoked prefrontal  $\gamma$  oscillations**

(A) Schematic showing the placement of EEG recording electrodes at the dorsolateral border of PFC in adult mice.

(B) Sample prefrontal EEG recordings from both adult *Dlx5/6<sup>+/-</sup>* and WT mice around the time of digging in the rule-shifting task; scale bars = 100  $\mu$ V, 100 msec.

(C) Log transform of the averaged, normalized power spectrum for prefrontal EEG recordings from *Dlx5/6<sup>+/-</sup>* (blue trace) and wild-type (black trace) mice. For this plot, the power spectrum from each mouse was normalized by the sum of all values from 0-120 Hz (excluding 58-62 Hz).

(D) Adult *Dlx5/6<sup>+/-</sup>* mice exhibit an increase in the power of prefrontal baseline  $\gamma$  (30-120 Hz) oscillations compared to their age-matched WT littermates.

(E) Change in unnormalized power (measured in log units) during the first ten trials of the rule-shifting portion of the task, compared to the baseline period, in 7-week old WT and *Dlx5/6*<sup>+/-</sup> mice. Task-evoked fast  $\gamma$  oscillations (62-120 Hz) are not significantly different between both genotypes.

(F) During periods of social interaction, both 7-week old wild-type and age-matched *Dlx5/6*<sup>+/-</sup> mice show a similar increase in prefrontal  $\gamma$  oscillations (compared to baseline).

(G) Task-evoked  $\gamma$  oscillations are significantly smaller in adult *Dlx5/6*<sup>+/-</sup> mice compared to age-matched WT littermates.

(H) During periods of social interaction, adult WT mice show an increase in the power of prefrontal  $\gamma$  oscillations (relative to baseline) compared to no change or a slight decrease in prefrontal  $\gamma$  power in age-matched *Dlx5/6*<sup>+/-</sup> mice.

To analyze changes in power during the baseline period (which was just before the social interaction task), we first used 2-way ANOVA and found significant effects of genotype ( $p < 0.001$ ), frequency ( $p < 0.001$ ), and genotype  $\times$  frequency ( $p < 0.05$ ). We then checked for differences between genotypes for each frequency band using two-tailed, unpaired Student's t-tests. For the rule-shifting task, we used repeated measures ANOVA with mouse, condition / time during task (baseline or time relative to digging), and genotype  $\times$  condition (baseline vs. task) as factors; asterisks indicate significance of the genotype  $\times$  condition interaction. For social interaction, we used repeated measures ANOVA with mouse, task condition (baseline vs. social interaction), and genotype  $\times$  condition (baseline vs. social interaction) as factors; asterisks indicate the significance of the genotype  $\times$  condition interaction.

All data show means  $\pm$  SEM and are analyzed using two-tailed Student's unpaired t-tests or 2-way ANOVA or repeated measures ANOVA. \*\* $p < 0.01$ , \*\*\* $p < 0.001$ .

See also Figure S4.

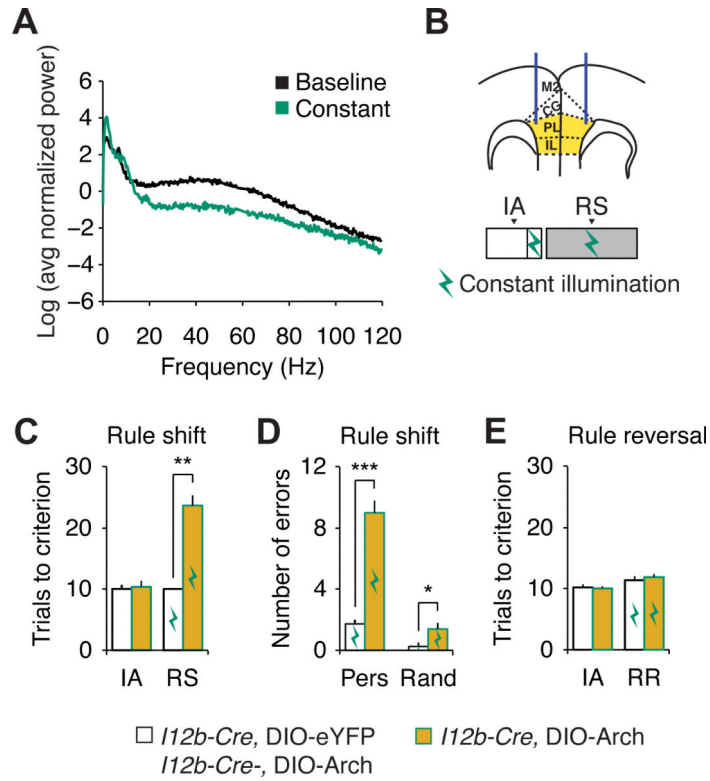


**Figure 5. Optogenetic inhibition of mPFC interneurons specifically disrupts rule shifts but not rule reversals**

(A) Optogenetic inhibition alters the power spectrum of prefrontal EEG activity recorded from the PFC of an adult *I12b-Cre* mouse while in its home cage, not performing any task. Note that for this plot, each power spectrum was normalized by the sum of all values from 0-120 Hz (excluding 58-62 Hz).

(B) Experimental design: we optogenetically inhibited interneurons by injecting Arch bilaterally into the PFC of *I12b-Cre* animals performing the IA and RS.

(C) During constant illumination, Arch-expressing *I12b-Cre* mice are impaired on the rule shift portion of the task compared with controls.

(D) While receiving optogenetic inhibition during the rule shift, Arch-expressing *I12b-Cre* mice make a preponderance of perseverative errors.

(E) Optogenetic inhibition of mPFC interneurons has no effect on rule reversal in Arch-expressing *I12b-Cre* mice compared to controls.

All data show means  $\pm$  SEM and are analyzed using two-tailed Student's t-tests or repeated measures ANOVA. \* $p < 0.05$ , \*\* $p < 0.01$ , \*\*\* $p < 0.001$ .

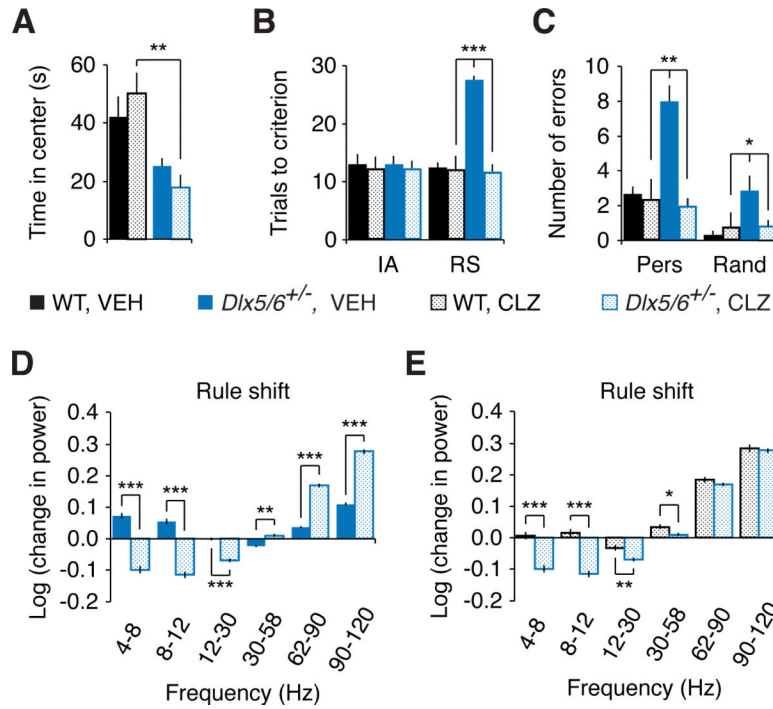


**Figure 6. Pharmacologic augmentation of interneuron function rescues cognitive inflexibility in adult *Dlx5/6*<sup>+/-</sup> mice**

(A) A single, I.P. injection of CLZ (0.0625 mg kg<sup>-1</sup>) did not significantly alter the time spent in the center of the open field by either adult *Dlx5/6*<sup>+/-</sup> mice or age-matched WT littermates.

(B) CLZ did not alter the number of trials needed to learn the initial association in either adult *Dlx5/6*<sup>+/-</sup> mice or age-matched WT littermates. However, CLZ completely normalized the number of trials required for adult *Dlx5/6*<sup>+/-</sup> mice to learn the rule-shifting task. The number of trials to learn the rule reversal was not affected.

(C) CLZ completely normalizes the number of errors made by adult *Dlx5/6*<sup>+/-</sup> mice during rule shifting.

(D) Task-evoked fast  $\gamma$  oscillations (62-120 Hz) in adult *Dlx5/6*<sup>+/-</sup> mice were significantly larger in CLZ than in vehicle.

(E) After CLZ treatment, task-evoked power in the 62-90 and 90-120 Hz bands was similar for adult *Dlx5/6*<sup>+/-</sup> and WT mice.

All data show means  $\pm$  SEM and are analyzed using two-tailed Student's t-tests or repeated measures ANOVA. \*p < 0.05, \*\*p < 0.01, \*\*\*p < 0.001.

See also Figure S5.



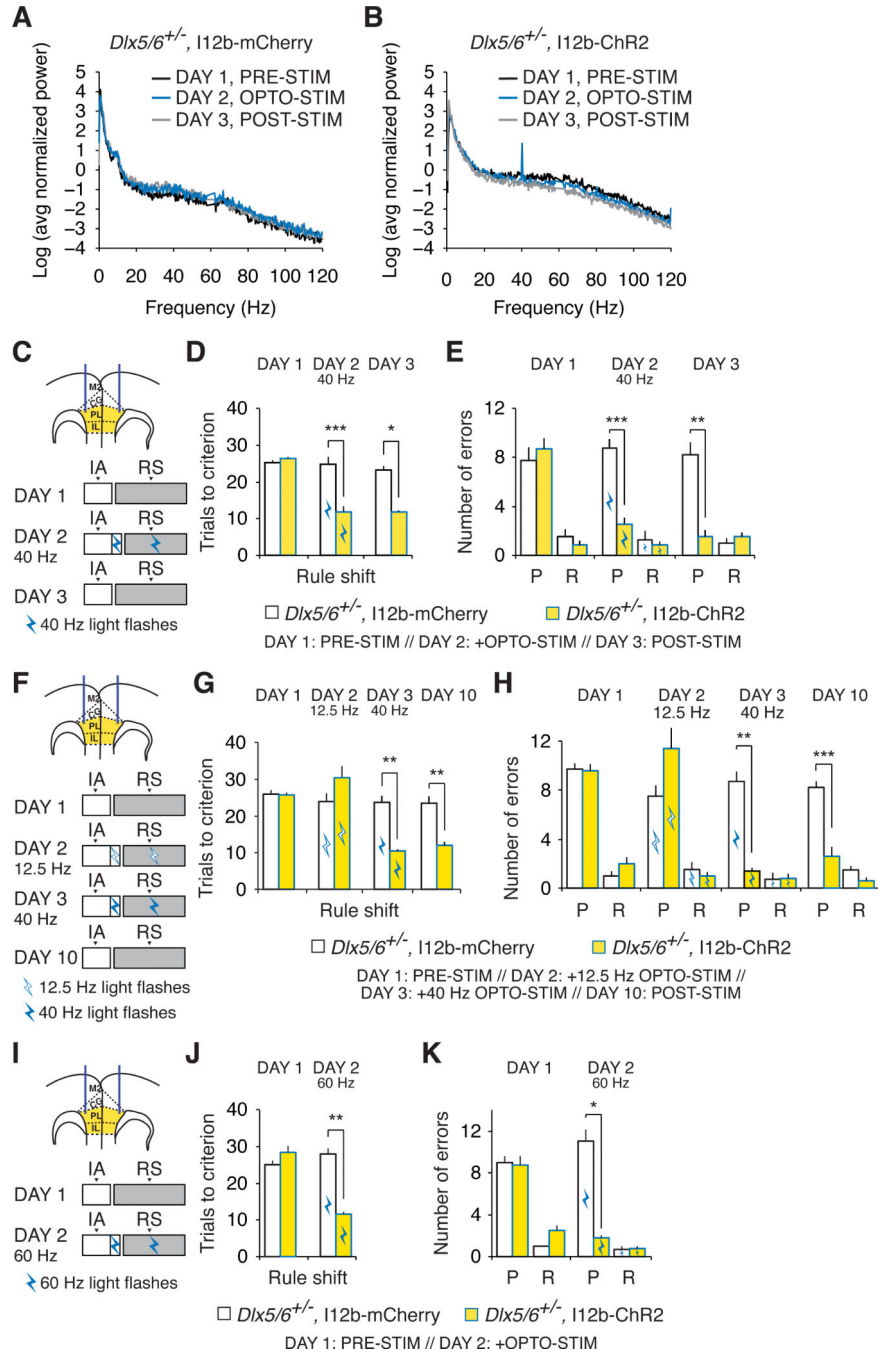


**Figure 7. Optogenetic augmentation of interneuron function rescues cognitive flexibility in adult *Dlx5/6<sup>+/-</sup>* mice**

(A) Log transform of the normalized power spectrum for prefrontal EEG recordings from an adult *Dlx5/6<sup>+/-</sup>* mouse injected with AAV-I12b-mCherry in the mPFC during the first ten trials of the rule shift portion of the task in the absence of light stimulation on Day 1, in the presence of optogenetic stimulation (40 Hz, 5 msec) on Day 2, and in the absence of light stimulation on Day 3. For this plot, the power spectrum from each mouse was normalized by the sum of all values from 0-200 Hz (excluding 58-62 Hz).

(B) Similar to (A) but shows power spectrum of prefrontal EEG recordings from an adult *Dlx5/6<sup>+/-</sup>* mouse injected with AAV-I12b-ChR2 in the mPFC.

(C) Schematic illustrating the design of experiments using 40 Hz optogenetic stimulation of mPFC interneurons during rule shifting. Dual fiber-optic cannulae were implanted bilaterally in the mPFC of *Dlx5/6<sup>+/-</sup>* mice. AAV (yellow) was also injected into the PFC bilaterally to drive expression of either ChR2-eYFP or mCherry in interneurons using the I12b enhancer. On Day 1, animals performed the initial association (IA) and rule shift (RS) in the absence of optogenetic stimulation. On Day 2, after the 80% correct criterion was reached in the IA, optogenetic stimulation was switched on, and continued during three additional IA trials and the subsequent RS. On Day 3, animals again performed the IA and RS in the absence of optogenetic stimulation. Optogenetic stimulation = blue light flashes at 40 Hz.

(D) Rule shift performance does not differ between *Dlx5/6<sup>+/-</sup>* mice that express ChR2 or mCherry in interneurons on Day 1, prior to optogenetic stimulation. However, 40 Hz stimulation on Day 2 selectively normalizes rule shifting in ChR2-expressing *Dlx5/6<sup>+/-</sup>* mice. *Dlx5/6<sup>+/-</sup>* mice that express ChR2 maintain improved cognitive flexibility on Day 3, even without additional light stimulation.

(E) The improved rule-shifting performance in (D) is accompanied by a decrease in perseverative errors (P).

(F) Similar to (C), the experimental design for experiments in which animals perform the IA and RS in the absence of optogenetic stimulation on Day 1, then receive 12.5 Hz optogenetic stimulation of PFC interneurons on Day 2, and 40 Hz optogenetic stimulation on Day 3.

(G and H) Unlike 40 Hz stimulation, the 12.5 Hz pattern of stimulation depicted in (F) fails to improve either the number of trials required to learn the rule shift (G). *Dlx5/6<sup>+/-</sup>* mice that express ChR2 maintain improved cognitive flexibility on Day 10 (i.e., 7 days after 40 Hz stimulation), even in the absence of additional light stimulation (G).

(I-K) 60 Hz optogenetic stimulation also improves learning of a rule shift and reduces perseverative errors in ChR2-expressing *Dlx5/6<sup>+/-</sup>* mice.

All data show means  $\pm$  SEM and are analyzed using two-tailed Student's t-tests or repeated measures ANOVA. \* $p < 0.05$ , \*\* $p < 0.01$ , \*\*\* $p < 0.001$ .

See also Figures S6 and S7.